Analysis methods for characterizing ferroelectric/ferroelastic domain reorientation in orthorhombic perovskite materials and application to Li-doped $Na_{0.5}K_{0.5}NbO_3$

Thanakorn Iamsasri · Goknur Tutuncu · Chunmanus Uthaisar · Soodkhet Pojprapai · Jacob L. Jones

Abstract Ferroelectric and ferroelastic domains can be reoriented during the application of electric field through domain wall motion. This study develops a method to quantify the domain reorientation in perovskite ferroelectrics with orthorhombic crystal lattices. In situ, high-energy X-ray diffraction was utilized to obtain intensity ratios that are necessary for the calculation. Domain reorientation in orthorhombic Li-doped $Na_{0.5}K_{0.5}NbO_3$ is then quantified using this method. The preference of domain orientations is explained by considering the angle between spontaneous polarization of the respective domains and the applied electric field direction. The extent of domain reorientation increases as the Li substitution increases which additionally correlates to increased piezoelectric coefficient d_{33} and field-induced strain. Increased domain wall motion is further proposed to originate due to the increased compositional proximity to the morphotropic phase boundary, a proposed universal behavior in ferroelectric compositions-containing phase boundaries.

T. Iamsasri · G. Tutuncu · J. L. Jones (✉)
Department of Materials Science and Engineering, University of Florida, Gainesville, FL 32611, USA
e-mail: jjones@mse.ufl.edu

C. Uthaisar · S. Pojprapai
School of Ceramic Engineering, Institute of Engineering, Suranaree University of Technology, Nakon Ratchasima 30000, Thailand

Introduction

Ferroelectrics are used in many applications and devices ranging from ferroelectric memories to high-strain actuators [1, 2]. In situ measurements of domain wall motion in ferroelectric materials have been provided by electro-optic imaging microscopy, X-ray microdiffraction, and X-ray diffraction from polycrystalline materials [3–7]. One benefit of X-ray diffraction is that intensities can be used to quantify the degree of preferred domain orientation and is thus able to measure changes in non-180° domain volume fractions during and after applied fields [4, 8–10]. Methods have been developed for transforming intensities of ferroelastic degenerate peaks into domain volume fractions in tetragonal and rhombohedral perovskites [4, 8–10]. Though domain wall motion in orthorhombic perovskite materials (i.e., space group *Amm*2) has been described qualitatively, however, quantitative relationships between intensities and domain volume fractions have not yet been developed for these materials [11]. Materials that exhibit this space group, such as $Na_{0.5}K_{0.5}NbO_3$ (NKN), have been rigorously investigated in a resurgence of research on lead-free materials and quantitative methods to describe domain wall motion are needed [12, 13].

The piezoelectric properties of $Na_yK_{1-y}NbO_3$ are maximum at approximately $y = 0.5$ [14]. In 2004, Saito et al. [15] highlighted the abilities of NKN solid solutions to achieve high-piezoelectric properties relative to lead-based ferroelectrics. The properties of unmodified NKN typically include a piezoelectric coefficient, d_{33}, of approximately 160 pC/N and a planar coupling coefficient, k_p, of 0.45 [14]. By doping with a certain amount of Li, the structure can be transformed from orthorhombic to tetragonal at room temperature, and the piezoelectric properties are enhanced near the morphotropic phase boundary

(MPB) [16]. The MPB of $(1-x)(Na_{0.5}K_{0.5})NbO_3–xLiNbO_3$ (100xLNKN) occurs between $x = 0.05-0.07$ [17]. The phase diagram of LNKN has been reported by Klein et al. [18].

This study develops a method to quantify the domain wall motion for orthorhombic ferroelectrics and applies the method to LNKN with compositions $x = 0.03-0.05$. Due to the proximity of these compositions to the MPB, a significant amount of domain wall motion is expected. The amount of domain wall motion as a function of Li content supports a hypothesis that Li enhances properties of NKN such as d_{33} through an increase in domain wall motion. This suggests that domain wall motion strongly affects the electromechanical behavior of LNKN.

Experiment

LNKN samples were prepared by a conventional mixed oxide method. The starting substances were powders of Nb_2O_5 (Sigma-Aldrich Co. 99.9 % purity), Na_2CO_3 (Sigma-Aldrich Co. 99.9 % purity), K_2CO_3 (Merck, 99 % purity), and $LiCO_3$ (Merck, 98.5 % purity). The powders were mixed with zirconia ball-milling media in ethanol for 24 h. The mixture was dried at 180 °C for 2 h. The dried mixture was ground and sieved to reduce the mixture particle size and screen the rough particles. The powder was calcined at 850 °C for 24 h. To prepare the green body, the powder was mixed with polyvinyl alcohol 5 vol% aqueous solution as an organic binder. After mixing, the rough particles of powder were screened again by using a 120 mesh sieve. Then, the fine powder was formed into a disk by using a uniaxial hydraulic pressing machine at 130 MPa and cold isostatic pressing machine at 250 MPa. The samples were sintered at 1190 °C with the heating rate of 5 °C/min in air for 2 h. The sintered LNKN specimens were successively polished using 800, 1200, 1800, and 2000 grit size SiC grinding papers. The samples were cut to approximate dimensions of $1.21 \times 1 \times 0.8$ mm^3, and after annealing at 600 °C for 4 h, they were gold sputtered and coated with silver electrode on opposing parallel surfaces. The density of all samples is more than 90 % of the theoretical density. The average grain size is about 1–2 μm. The phase purity of samples is confirmed by X-ray diffraction.

Diffraction patterns were measured during the application of electric fields using high-energy X-rays at beamline 11-ID-C of the Advanced Photon Source, Argonne National Laboratory. The X-ray beam had a wavelength of 0.10798 Å and size of 0.5×0.5 mm. The diffraction patterns were measured in forward scattering geometry using a Perkin Elmer area detector at a distance of approximately 2250 mm. The samples were subjected to an

electric field amplitude of 2 kV/mm utilizing a triangular bipolar waveform with a frequency of 0.125 Hz. The amplitude of electric field was increased to 2.5 kV/mm for a second cycle. The field amplitudes of both cycles are above the coercive field of LNKN.

Results and discussion

The structure of 100xLNKN, where $0 < x < 5$, can be described by using an orthorhombic or pseudo-monoclinic reference frame (the latter of which involves lattice parameters $a_M = c_M$). The equivalent plane indices for certain reflections of these two reference frames are listed in Table 1. The possible polarization axes in orthorhombic perovskite materials are in the $\langle 110 \rangle_M$ directions, where M indicates the pseudo-monoclinic cell, as shown in Fig. 1, [19]. Recently, Ge et al. [20] have shown that 5LNKN may have a monoclinic structure which is different from the pseudo-monoclinic structure that equally describes the orthorhombic phase. The structure reported by Ge et al. includes an additional lattice distortion of the perovskite structure involving the expansion of lattice parameter a_M and the contraction of lattice parameter c_M so that $a_M \neq c_M$. Reference to the pseudo-monoclinic unit cell (M) in this study hereafter refers to the former definition, in which $a_M = c_M$. The quantification and analysis of the degree of domain reorientation in monoclinic crystal structures are complicated since the monoclinic unit cell has an infinite number of possible polarization directions. For simplicity, therefore, we develop equations in this study for the orthorhombic case which may, in certain instances, apply equally to pseudo-monoclinic unit cells. To confirm the different levels of Li substitution, the lattice parameters of relevant LNKN compositions with respect to the orthorhombic reference frame are calculated from the X-ray diffraction patterns and are shown in Table 2.

For orthorhombic LNKN, the spontaneous polarization vector is parallel to the c-direction of the unit cell. The diffracting planes reported in this study are approximately perpendicular to the applied electric field. When the electric field is applied, the domains reorient such that the domain orientations with polarization vectors most closely parallel to the electric field are preferred relative to the

Table 1 Indices for $\{220\}_M$ reflections with respect to pseudo-monoclinic and orthorhombic reference frame

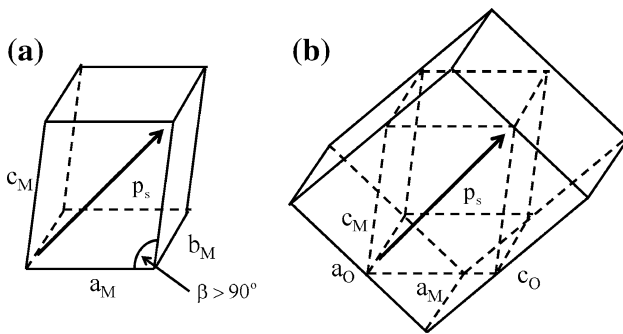| Pseudo-monoclinic	Orthorhombic	2θ (degrees)	d-Spacing (Å)
$(202)_M$	$(004)_O$	4.36	1.42
$(022)_M$	$(400)_O$	4.39	1.41
$(220)_M$	$(222)_O$	4.41	1.40

Fig. 1 Spontaneous polarization direction in orthorhombic LNKN with respect to **a** pseudo-monoclinic cell and **b** orthorhombic unit cell

Table 2 Lattice parameters of LNKN with respect to orthorhombic reference frame

Composition	a (Å)	b (Å)	c (Å)
3LNKN	5.644	3.945	5.679
4LNKN	5.644	3.942	5.680
5LNKN	5.640	3.941	5.679

other domain orientations. Domain reorientation is therefore expected to be measurable in the $\{hh0\}_M$ reflections because they correspond to domains with polarization axes parallel and perpendicular to the electric field direction. However, for orthorhombic LNKN, the $\{110\}_M$ reflections are only clearly split into two measurable peaks which are insufficient to quantify the degree of domain reorientation between three variants. The $\{220\}_M$ reflections, which are parallel to the $\{110\}_M$ reflections, split into three resolved peaks because of larger peak splitting at higher 2θ angles. Thus, the $\{220\}_M$ reflections are used to quantify the domain reorientation in this study.

The vertical sector of two-dimensional X-ray diffraction patterns, which measures scattering vectors approximately parallel to the electric field direction, was integrated by Fit2d software using $\pm7.5°$ azimuthal angles [3, 4]. Figure 2 shows the $\{220\}_M$ reflections with crystallographic poles parallel to the electric field direction during the application of triangular bipolar waveform with amplitude 2 kV/mm and time period 80 s on unpoled 3LNKN, 4LNKN, and 5LNKN. The intensity change in the $\{220\}_M$ reflections with applied electric field indicates changes in non-180° domain volume fractions. At an electric field amplitude of approximately 1.5 kV/mm, the intensity of the $(202)_M$ reflection increases while the intensity of the $(220)_M$ reflection decreases significantly. The integrated intensity of individual $\{220\}_M$ reflections was obtained by fitting the measured intensity profile to three symmetric Gaussian functions with a constraint that the $(022)_M$ reflection and the $(220)_M$ reflection have the same full width at half maximum. This constraint was

found to be necessary to enable reliable convergence of the fit and is justified on the basis that microstructural and instrumental broadening should not be significantly different for these diffraction peaks. Figure 3 shows representative data measured at a field amplitude of 2 kV/mm, including the measured intensity, the component Gaussian profile fits, the overall fit, and the difference between the measured and overall fit.

In 1957, Subbarao et al. [8] developed an equation to quantify the reorientation of domains in tetragonal BaTiO$_3$ under applied stress, and several authors have since quantified the domain switching in tetragonal and rhombohedral structures under applied electric field using similar formulae [4, 9, 10]. However, quantification methods of domain reorientation for orthorhombic perovskite materials have not been developed. This study presents a quantification method leading to a value called the *fraction of domain interchange*, the detailed derivation of which can be found in the supplementary material. The intensity from domain orientations corresponding to any of the diffraction peaks can change to other peaks during the application of electric field. The intensity changes can be used to determine the fraction of domain interchange from peak i to peak j (n_{i-j}). For orthorhombic perovskite materials, n_{i-j} for the $\{220\}_M$ reflections is defined as

$$n_{i-j} = \frac{-R_i + R_j}{R_{202} + R_{022} + R_{220}}, \tag{1}$$

where $i, j = 202, 022$, or 220, $i \neq j$, and R_i is the ratio of integrated intensity during application of electric field to integrated intensity of the peak i from the unpoled sample. The fraction of domain interchange scales from -1 to 1, and n_{i-j} is equal to $-n_{j-i}$. If the value of n_{i-j} is positive, the domains corresponding to peak i reorient to domains corresponding to peak j.

Using this method, Fig. 4 shows the fraction of domain interchange for 3LNKN, 4LNKN, and 5LNKN during the application of a triangular bipolar waveform of amplitude 2.5 kV/mm and time period 80 s. The fraction of domain interchange is hysteretic because of the irreversible motion of domain walls. From Fig. 4, $n_{022-202}$ and $n_{220-202}$ values are positive while $n_{220-022}$ is negative. These results indicate that the domains corresponding to the $(022)_M$ reflection reorient to the domains corresponding to the $(202)_M$ reflection and the $(220)_M$ reflection, while domains corresponding to the $(220)_M$ reflection reorient to the domains corresponding to the $(202)_M$ reflection. These results agree qualitatively with the diffraction patterns shown in Fig. 2, which show that the intensity of $(202)_M$ increases and the intensity of $(022)_M$ decreases after application of electric field. After the electric field is applied, the domains can be listed from the most to the least preferred orientation as follows: $(202)_M$, $(220)_M$, and $(022)_M$.
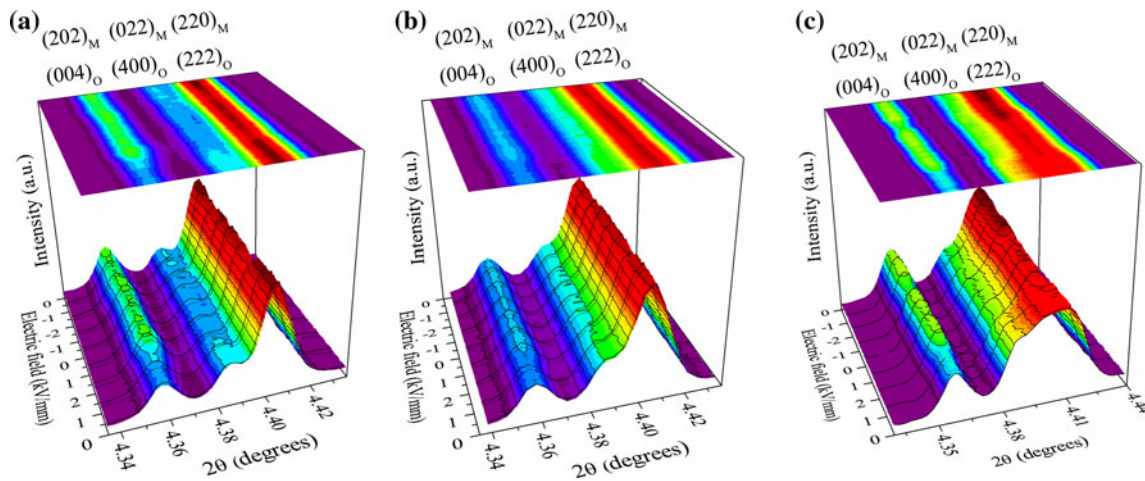
Fig. 2 The $\{220\}_M$ reflections with crystallographic poles parallel to the electric field direction during the first application of triangular bipolar waveform on unpoled **a** 3LNKN, **b** 4LNKN, and **c** 5LNKN samples
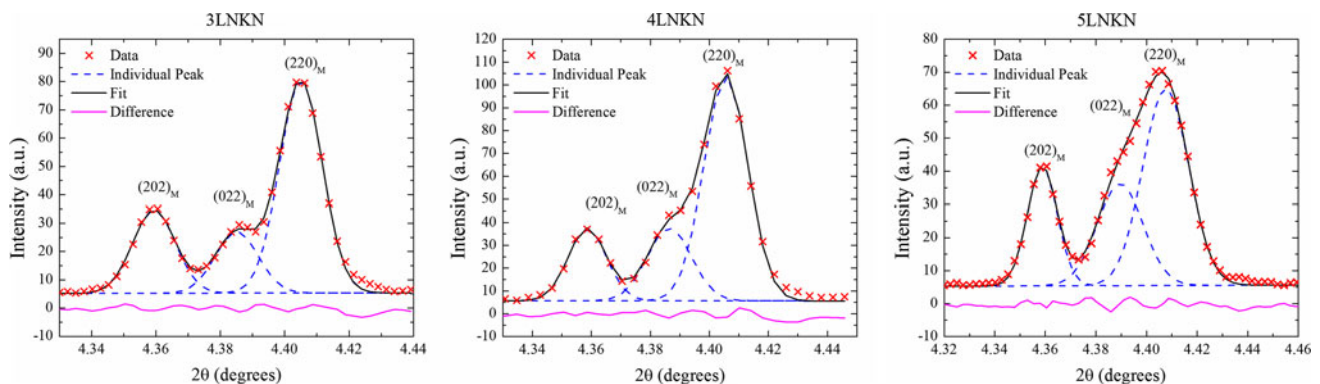

Fig. 3 Measured intensity, Gaussian profile fits, the overall fit, and difference between the measured and overall fit of $\{220\}_M$ reflections of 3LNKN, 4LNKN, and 5LNKN at 2 kV/mm

The lattice parameters of orthorhombic NKN have been reported as $a_O = 5.6395$ Å, $b_O = 3.9399$ Å, and $c_O = 5.6725$ Å and are nearly constant in the range $x = 0-0.05$ [17, 21]. The lattice parameters of the corresponding pseudo-monoclinic cell are $a_M = c_M = 4.000$ Å, $b_M = 3.940$ Å, and $\beta = 90.34°$. The possible polarization axes are in the $\langle 110 \rangle_M$ directions of a pseudo-monoclinic cell where the spontaneous polarization vector is parallel to c_O as shown in Fig. 1. Figure 5 shows the spontaneous polarization vectors for each plane of the $\{220\}_M$ reflections. In this study, the applied electric field is always approximately perpendicular to the diffracting planes, but the spontaneous polarization directions are different for each domain. The spontaneous polarization vector and the applied electric field are parallel in the domains corresponding to the $(202)_M$ plane, perpendicular in the domains corresponding to the $(022)_M$ plane, and at a 60.34° angle in the domains corresponding to the $(220)_M$ plane. After the electric field is applied, the domains reorient to have polarization vector as closely as possible to the electric

field. This means that the domains corresponding to the $(202)_M$ reflection are the most preferred, the $(220)_M$ reflection are the second most preferred, and the $(002)_M$ reflection are the least preferred. The measured intensities correspond to this expectation based on the angle between the polarization direction and the applied electric field direction.

Results from Lai et al. and Wang et al. [13, 22] showed that d_{33} and field-induced strain of LNKN increase as Li content increases for $x = 0-0.06$. From Fig. 4, it can be seen that the values of fraction of domain interchange (n_{i-j}) also increase as Li content increases. Thus, domain wall motion can be considered as one of the possible mechanisms, which enhances the field-induced strain of LNKN. It should be noted that the domain wall motion during application of low-frequency or static electric fields of strong amplitude is strictly a distinctly different loading scenario from domain wall motion during application of cyclic, weak-electric field amplitudes such as those applied during measurement of piezoelectric properties. However,
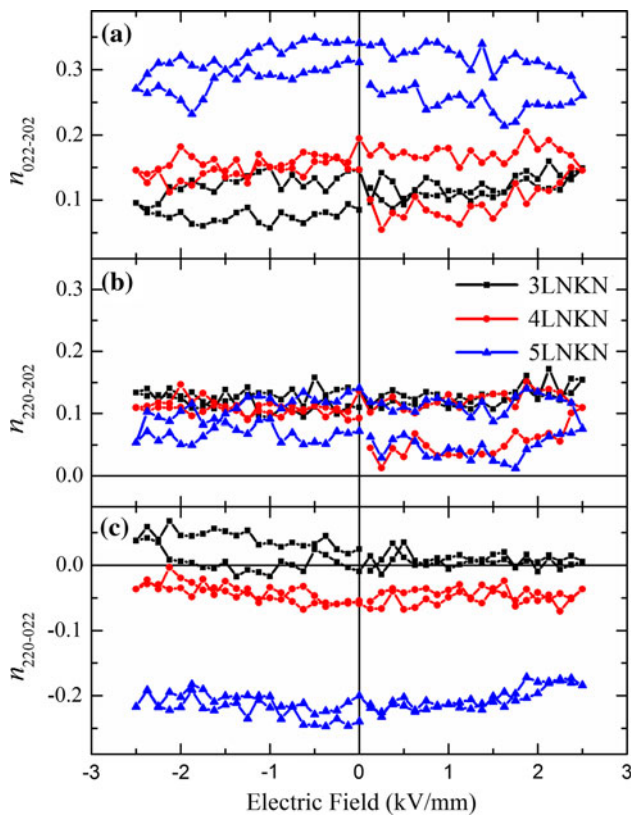
Fig. 4 Fraction of domain interchange of 3LNKN, 4LNKN, and 5LNKN during the application of triangular bipolar waveform with amplitude 2.5 kV/mm and time period 80 s
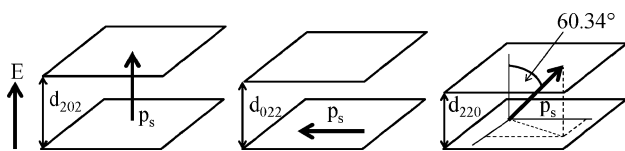

Fig. 5 Schematic of spontaneous polarization vectors in the $\{220\}_M$ planes

a high degree of domain wall motion during application of strong-electric fields is typically related to high mobility of domain walls during subcoercive field application, e.g., as observed in donor-modified lead zirconate titanate in which a large contribution of domain wall displacement to field-induced strain and piezoelectric coefficients is observed [23]. Thus, the increase in domain wall motion observed during application of high-electric fields in this study may be correlated with an equivalent enhancement in domain wall contributions to the piezoelectric coefficients. The degree of domain wall motion during electrical poling has also been previously correlated with enhanced piezoelectric coefficients in other ferroelectric ceramic materials, e.g., as has reported in orthorhombic-structured Aurivillius phases [24]. In this study, the substantial increase of domain wall motion seen with Li substitution may be

considered to be due to either a fundamental change in the way in which the substituent (i.e., Li) interacts with domain walls, or the movement of the composition closer to the MPB. In considering the first possibility (substituents interacting with domain walls), we note that Li substitution in NKN is isovalent and it is not expected to generate other point defects to compensate for charge. Thus, Li substitution is dissimilar to acceptor and donor doping which are common approaches to modify domain wall mobility and generate hard and soft ferroelectric behavior in Pb-based perovskites. It is therefore unlikely that Li or any other newly generated defect substantially affects the mobility or pinning of domain walls. We therefore return to the possibility that Li substitution enhances domain wall motion by changing the compositional proximity to the phase boundary. In $PbZr_xTi_{1-x}O_3$ (PZT), it has been shown that domain wall motion increases as the MPB is approached [23]. Thus, the enhancement in domain reorientation that is observed in LNKN with increasing Li concentration may also be considered to be due to increased compositional proximity to the phase boundary. This result provides additional evidence for an emerging universality in perovskite ferroelectric materials that domain wall motion increases with increasing proximity to phase boundaries.

Conclusions

This study presents a method to quantify domain switching in orthorhombic structured materials that lead to a value called fraction of domain interchange. The method is applied to several orthorhombic compositions of Li-substituted NKN ferroelectric materials. The domains corresponding to the $(202)_M$ reflections were found to be the most preferred during electric field application, the domains corresponding to the $(220)_M$ reflections were found to be the second most preferred, and the domains corresponding to the $(022)_M$ reflections were found to be the least preferred. The preference of domain orientations is explained by the angle between the spontaneous polarization in each domain and the electric field direction. The fraction of domain interchange increases as Li content increases, which corresponds to higher d_{33} and field-induced strain. The fact that domain wall motion increases significantly by Li substitution is attributed to the increasing compositional proximity to the phase boundary with increasing Li concentration.

References

1. Scott JF, Paz de Araujo CA (1989) Science 246:1400
2. Park SE, Shrout TR (1997) J Appl Phys 82:1804
3. Tutuncu G, Damjanovic D, Chen J, Jones JL (2012) Phys Rev Lett 108:177601
4. Pramanick A, Daniels JE, Jones JL (2009) J Am Ceram Soc 92:2300
5. Gopalan V, Mitchell TE (1999) J Appl Phys 85:2304
6. Grigoriev A, Do DH, Kim DM, Eom CB, Adams B, Dufresne EM, Evans PG (2006) Phys Rev Lett 96:187601
7. Pojprapai S, Russell J, Man H, Jones JL, Daniels JE, Hoffman M (2009) Acta Mater 57:3932
8. Subbarao EC, McQuarrie MC, Buessem WR (1957) J Appl Phys 28:1194
9. Bedoya C, Muller C, Baudour JL, Madigou V, Anne M, Roubin M (2000) Mater Sci Eng B 75:43
10. Jones JL, Slamovich EB, Bowman KJ (2005) J Appl Phys 97:034113
11. Hall DA, Azough F, Middleton-Stewart N, Cernik RJ, Freer R, Mori T, Kungl H, Curfs C (2010) Funct Mater Lett 03:31
12. Tutuncu G, Chang Y, Poterala S, Messing GL, Jones JL (2012) J Am Ceram Soc 95:2653
13. Lai F, Li JF, Zhu ZX, Xu Y (2009) J Appl Phys 106:064101
14. Jaeger RE, Egerton L (1962) J Am Ceram Soc 45:209
15. Saito Y, Takao H, Tani T, Nonoyama T, Takatori K, Homma T, Nagaya T, Nakamura M (2004) Nature 432:84
16. Guo Y, Kakimoto KI, Ohsato H (2004) Appl Phys Lett 85:4121
17. Sun X, Deng J, Chen J, Sun C, Xing X (2009) J Am Ceram Soc 92:3033
18. Klein N, Hollenstein E, Damjanovic D, Trodahl HJ, Setter N, Kuball M (2007) J Appl Phys 102:014112
19. Jaffe B, Cook WR, Jaffe H (1971) Piezoelectric Ceramics. Academic, New York
20. Ge W, Ren Y, Zhang J, Devreugd CP, Li J, Viehland D (2012) J Appl Phys 111:103503
21. Wu L, Zhang JL, Wang CL, Li JC (2008) J Appl Phys 103:084116
22. Wang K, Li JF (2007) Appl Phys Lett 91:262902
23. Pramanick A, Damjanovic D, Daniels JE, Nino JC, Jones JL (2011) J Am Ceram Soc 94:293
24. Jones JL, Slamovich EB, Bowman KJ, Lupascu DC (2005) J Appl Phys 98:104102